Available online at www.sciencedirect.com
ScienceDirect
Composites Science and Technology 67 (2007) 3409–3416
COMPOSITES SCIENCE AND TECHNOLOGY
www.elsevier.com/locate/compscitech

Characterization, fluoride release and recharge properties of polymer–kaolinite nanocomposite resins

Yin-Lin Wang [a], Bor-Shiunn Lee [a], Kai-Chun Chang [b], Hsin-Chuan Chiu [a], Feng-Huei Lin [b], Chun-Pin Lin [a,*]

[a] *School of Dentistry and Graduate Institute of Clinical Dentistry, College of Medicine, National Taiwan University and National Taiwan University Hospital, Taipei, Taiwan*
[b] *Institute of Biomedical Engineering, College of Medicine, National Taiwan University, Taipei, Taiwan*

Received 15 October 2006; received in revised form 8 March 2007; accepted 14 March 2007
Available online 24 March 2007

Abstract

Dental restorative composite resins with effective fluoride release and recharge properties have yet to be developed. In this study, we developed three types of polymer–kaolinite nanocomposite resins (C(K-diamine), C(K-acrylamide), and C(K-acetate)) with the potential to provide sustained release of fluoride due to the strong adsorption of kaolinite to fluoride during the fabrication process. Their mechanical (hardness, flexural strength, flexural modulus, fracture toughness, and diametral tensile strength) and fluoride release properties were investigated. X-ray diffraction (XRD) and Fourier transform infrared spectroscopy (FTIR) analyses demonstrated that hexanediamine, acrylamide, and ammonium acetate were successfully intercalated into the interlamellar structure of all three resins. Of the three types of polymer–kaolinite nanocomposite resins, C(K-acrylamide) exhibited the greatest mechanical strength and greater fluoride release than Fuji IX. In addition, C(K-acrylamide) released more fluoride than Fuji IX and Z-100 after exposure to 0.2% NaF. It is concluded that C(K-acrylamide) can potentially serve as a useful restorative material with caries-preventive properties.

Keywords: A. Particle-reinforced composites; Fluoride release; B. Mechanical property; C. Infrared spectroscopy; D. X-ray diffraction

1. Introduction

With the growing demand for esthetics in dentistry, tooth-colored restorations have been increasingly used in restoring cavities in preference to conventional amalgam fillings or gold restorations. Direct tooth-colored restorative materials that have been widely used include glass ionomer cements (GICs), resin-modified glass ionomer cements (RMGICs), compomers, and composite resins. GICs and RMGICs exhibit higher fluoride release and uptake capacity over a longer period of time than composite resins [1–3] but their compressive strengths are inferior [4]. The differences in compressive strengths were attributed to the gel network formed by acid–base reaction in glass ionomers, which generally had lower strength and toughness than crosslinked polymers of Bis-GMA, UEDMA and TEGMA in composite resins [4]. This has limited the clinical application of GICs and RMGICs to nonload-bearing sites. By contrast, composite resins and some compomers have relatively high mechanical strengths but their fluoride release abilities are limited [5,6]. Thus, the development of new materials with improved mechanical strength, high fluoride release and recharge ability is an important goal.

Fluoride release of restorative materials is generally considered to inhibit tooth demineralization and caries development, and also to strengthen the neighboring enamel or dentin [7–9]. Mechanisms that have been proposed for these effects include the formation of low soluble fluorapatite, remineralization enhancement, as well as inhibition of microbial metabolism and growth [10]. The higher concentration of fluoride leads to an increase in the amount

* Corresponding author. Tel.: +886 2 23123456x7335; fax: +886 2 23831346.
E-mail address: pinlin@ntu.edu.tw (C.-P. Lin).

0266-3538/$ - see front matter © 2007 Elsevier Ltd. All rights reserved.
doi:10.1016/j.compscitech.2007.03.018

of CaF_2 formed while a relatively low concentration of fluoride produces fluoridated apatite [11]. Although both compounds inhibit caries progression, fluoridated apatite formation is more desirable than CaF_2 as the former is more resistant to acid attack [12]. Kaolinite ($Al_2Si_2O_5(OH)_4$) has been suggested as an active substrate for de-fluoridation [13]. The high adsorption of kaolinite to fluoride is due to its layered aluminosilicate structure and high surface area [14]. In this study, we aimed to develop a dental restorative composite resin with high fluoride release and recharge properties. Three types of polymer–kaolinite nanocomposite resins were produced using kaolinite–hexanediamine (K-diamine), kaolinite–acrylamide (K-acrylamide), or kaolinite–ammonium acetate (K-acetate) as the inorganic filler. Due to the strong adsorption of kaolinite to fluoride, the fabricated nanocomposite resins could store and release more fluoride over a long period of time in comparison to GICs. The interlamellar space of kaolinite intercalated by hexanediamine, acrylamide, and ammonium acetate was also investigated using X-ray diffraction (XRD) and Fourier transform infrared spectroscopy (FTIR) analysis. Finally, the mechanical properties of the fabricated nanocomposite resins including microhardness, flexural strength, flexural modulus, fracture toughness, and diametral tensile strength were analyzed.

2. Experiment

2.1. Preparation of kaolinite/N-methylformamide (K-NMF) and kaolinite/dimethyl sulfoxide (K-DMSO) filler

Five g of raw kaolinite (Fluka Chemie, Buchs, Switzerland) was transferred to a 250-ml flask and suspended in 60 ml of *N*-methylformamide (NMF) (Sigma–Aldrich Co., St. Louis, USA) containing 5 ml of distilled water. The suspension was stirred on a magnetic stir plate at room temperature for 72 h and then centrifuged at 4000 rpm (L-7 ultracentrifuge, Beckman Instruments Inc., Palo Alto, CA) for 10 min to recover the solids and discard the supernatant. The resulting material was then lyophilized for 48 h (Labconco Freeze Dryer, Kansas City, MO) to obtain K-NMF filler.

For K-DMSO filler, 9 g of raw kaolinite was transferred to a 250-ml flask and suspended in 60 ml of DMSO (Sigma–Aldrich Co., St. Louis, USA) containing 5.5 ml of distilled water. The suspension was stirred at 60 °C for 72 h. The solution was centrifuged and lyophilized using the same method as for K-NMF filler.

2.2. Preparation of fluoride-releasing K-diamine, K-acrylamide, and K-acetate filler

Three g of K-NMF and 5 g of hexanediamine (Sigma–Aldrich Co., St. Louis, USA) were mixed with 100 ml deionized water and stirred at room temperature for 72 h. Subsequently, 0.5 g of NaF and 10 ml of 5 M $NaNO_3$ buffer were added and the pH value was adjusted to 4 by titration of 12 M HCl or 1 M NaOH. The solution was stirred again at room temperature for 24 h and centrifuged at 4000 rpm for 10 min to remove the supernatant. Finally, the remaining mixture was lyophilized for 48 h to obtain fluoride-releasing K-diamine filler.

For K-acrylamide filler, 2 g of K-NMF and 12 g of acrylamide (Sigma–Aldrich Co., St. Louis, USA) were mixed with 88 ml deionized water to obtain 12 wt% of acrylamide solution. The mixture was stirred at room temperature for 24 h. The other procedures were the same as for fluoride-releasing K-diamine filler.

For K-acetate filler, 2 g of K-DMSO and 36 ml of ammonium acetate (Sigma–Aldrich Co., St. Louis, USA) were mixed with 24 ml deionized water to obtain 60 wt% of ammonium acetate solution. The other procedures were the same as for fluoride-releasing K-acrylamide filler.

2.3. Preparation of fluoride releasing nanocomposite resin

Light curable nanocomposite resin was prepared by mixing 2,2-bis[4-(3-methacryloxy-2-hydroxypropoxy) phenyl] propane (Bis-GMA), triethyleneglycoldimethacrylate (TEGDMA), *N*,*N*-dimethyl-*p*-toluidine (DMPT), and camphorquinone (CQ) in the weight ratio of 70:30:0.5:0.5. All materials were purchased from Sigma. Fifty wt% of K-diamine, K-acrylamide, or K-acetate filler was added into the polymer matrix to obtain three types of fluoride-releasing nanocomposite resins (C(K-diamine), C(K-acrylamide), and C(K-acetate)). In our pilot study, 50 wt% of filler was the concentration at which the resins exhibited the best mechanical properties. The uncured composite resin was placed into a polytetrafluoroethylene (PTFE) mold (6 mm in diameter and 2 mm in thickness), covered with a Mylar matrix, and light cured with a light-emitting diode (LED) light-curing unit (LEDemetron II, SDS Kerr, Danbury, CT, USA) for 40 s from the top and bottom sides, respectively. The energy output was 750 mW/cm^2 calibrated with a power meter (Cure Rite, Caulk Dentsply, Milford, DE, USA).

2.4. Analysis and testing

2.4.1. X-ray diffraction (XRD) analysis

To investigate the penetration of the gallery space (intercalation) of kaolinite by hexanediamine, acrylamide, or ammonium acetate, the crystalline phases and *d*-spacing of the specimens were determined by a Rigaku X-ray powder diffractometer (Rigaku Denki Co., Ltd., Tokyo, Japan) with Cu Kα radiation and Ni filter. The scanning range was from 10° to 60° with a scanning speed of 4°/min. To determine the contents of different phases, relative intensities of the characteristic peaks of each phase were used.

2.4.2. Fourier transform infrared spectroscopy (FTIR) analysis

To investigate the changes of functional groups after intercalation, specimens were studied with Fourier trans-

form infrared spectroscopy (FTIR). The FTIR spectra were recorded using KBr pellets (1 mg sample per 300 mg KBr) on a Jasco FTIR grating instrument (FTIR-300E, Jasco International Co. Ltd., Tokyo, Japan) with slow scan and normal slit width. The wavelength used was in the range of 4000–400 cm^{-1}.

The degree of polymerization (DP) was investigated with FTIR. The intensities of the aliphatic C=C absorbance peak at 1645 cm^{-1} and the aromatic C=C absorbance peak at 1617 cm^{-1} were measured. Subsequently, the ratio of the absorbance intensities of aliphatic C=C/aromatic C=C was compared before and after polymerization using the following equation [15]:

$$\mathrm{DP}\ (\%) = 100 - \frac{[\text{aliphatic (C=C) abs./aromatic (C=C) abs.}]_{\text{after cure}}}{[\text{aliphatic (C=C) abs./aromatic (C=C) abs.}]_{\text{before cure}}} \times 100 \quad (1)$$

2.4.3. Hardness test

Ten specimens from each of the three types of nanocomposite resins and a conventional composite resin (Z-100, 3M ESPE, St. Paul, MN, USA) were prepared for evaluation using a hardness tester (SHIMADZU HMV-2, Japan). Z-100 is composed of Bis-GMA, TEGDMA, CQ, ethyl 4-dimethyl amino benzoate (EDMAB), silanated zirconia, and silica. Before testing, the specimen surfaces were wet-ground with 1000-grit silicon carbide paper at room temperature. The Knoop hardness test was performed using a diamond indenter with 0.2 kg load and 40 s dwell time. Five measurements were made on the surface of each specimen and the mean value was considered as the hardness. Ten mean values of 10 specimens in each group were calculated again to obtain the final mean value and the standard deviation of hardness. The data for the three types of nanocomposite resins and Z-100 were analyzed using one-way ANOVA and post-hoc test (Tukey's) with the level of significance set at 5%.

20 mm distance between supports to ensure an equally distributed load [16] and measured with a universal testing machine (Instron Corp, Canton, MA, USA) at a crosshead speed of 0.5 mm/min. The flexural strength (α) and flexural modulus (E_B) were calculated using the following formulas:

$$\alpha = \frac{3FL}{2bh^2} \quad (2)$$

$$E_B = \frac{L^3 m}{4bh^3} \quad (3)$$

where F = load (kN), L = span (cm), h = specimen depth (cm), b = specimen width (cm), m = slope of the tangent to the initial straight-line portion of the load–deflection curve.

Fracture toughness (K_{1C}) was determined according to ASTM Designation E 399-83, using 10 single-edge notched-bend specimens of each material. The specimens ($16 \times 2 \times 2$ mm) were made and polymerized as described above. A notch ($0.5 \times 2 \times 1$ mm) was machined into each specimen with a diamond saw (Proxxon, Hermann, Tonisvorst, Germany) using water coolant. The specimens were then loaded to fracture on another 3-point bending test device (span $S = 12$ mm distance between the supports) with the same universal testing machine (cross-head speed 0.5 mm/min) at room temperature. Load–deflection (P = load) curves were recorded. The heights (B) and the widths (W) of the specimens were measured with a micrometer and the notch depths (a) were determined with a measuring microscope. K_{1C} was calculated from measurements with the single-edge notched-bend specimens using the relation [17,18]:

$$K_{1C} = \frac{PS \times 3(a/W)^{1/2}[1.99 - (a/W)(1 - a/W) \times (2.15 - 3.93a/W + 2.7(a^2/W^2))]}{BW^{3/2}2(1 + 2a/W)(1 - a/W)^{3/2}} \quad (4)$$

2.4.4. Flexural strength, flexural modulus, fracture toughness, and diametral tensile strength measurements

Flexural strength and flexural modulus were determined according to ISO 4049. Ten specimens of each of the three types of nanocomposite resins and Z-100 were made by inserting the composite material into a PTFE mold ($25 \times 2 \times 2$ mm), covering the surfaces with a Mylar matrix, and curing with the LED curing unit. The specimens were placed on a 3-point bending test device with

Ten specimens of each of the three types of nanocomposite resins and Z-100 were tested for the diametral tensile strength. Cylindrical specimens were prepared in PTFE molds (3 mm high, 6 mm diameter) and polymerized as described above. Diametral tensile strength was then measured using a universal testing machine at 10 mm/min cross-head speed and calculated as $2P/\pi DT$, where P = load at fracture; D = diameter; and T = thickness [19].

2.4.5. Fluoride release measurement

The fluoride release and recharge properties of the following five materials were measured: C(K-diamine), C(K-acrylamide), C(K-acetate), a highly viscous conventional glass ionomer (Fuji IX GP, GC Co., Tokyo, Japan), and Z-100. Fuji IX is composed of alumino-fluorosilicate glass, polyacrilic acid powder, pigments, water, polyacrilic acid, and polybasic carboxylic acid. Twenty specimens of each of the five materials were made by inserting the composite material into a PTFE mold (diameter: 6 mm; thickness: 2 mm) and polymerized as above. A continuous flow apparatus was used for the measurement of fluoride release [20]. Briefly, each test disc was suspended in the drip chamber filled with 3 ml of deionized water. At designated time points (4, 8 h; 1, 2, 3, 4, 5, 6, 7, 14, 28, 42, and 56 days) 0.5 ml of solution in the drip chamber was transferred into a plastic micro-centrifuge tube. Immediately after withdrawal of the solution, 0.5 ml of deionized water was added to the chamber to maintain the water volume at 3 ml. The solutions collected from the drip chamber were buffered with an equal volume of diluted TISAB III (concentrated Total Ionic Strength Adjustment Buffer, 94-09-11, Orion Research Inc., MA, USA). The fluoride content was then measured using a microanalytical technique with an inverted fluoride-specific electrode (Fluoride electrode, lot no. 9409, Orion Research Inc., USA) [21] and calculated using the following equation:

$$\begin{aligned}\mu\text{g F/cm}^2 &= \text{ppm F}(\mu\text{g F/mL}) \\ &\times \text{mL}(\text{volume of medium at unit time}) \\ &\times 1/\text{surface area of specimen} \end{aligned} \quad (5)$$

After a 56-day period of fluoride release, 10 specimens from each of the five materials were re-immersed in 5 ml, 0.2% NaF solution at pH 7 for 1 min and the other 10 specimens were re-immersed in 5 ml, 0.2% NaF solution at pH 4 for 1 min. The fluoride content was then measured again at the same designated time points. Statistical analysis was performed using the Kruskal–Wallis test (significant level of 5%, for non-parametric data on cumulative fluoride release) followed by Mann–Whitney *U* test (significant level of 5%, for multiple comparison).

3. Results and discussion

3.1. XRD and FTIR analyses

In this study, we used kaolinite ($Al_2Si_2O_5(OH)_4$) for intercalation reactions because it is a layered aluminosilicate of the 1:1 type that is formed by two different types of interlayer surfaces. Aluminum atoms coordinate octahedrically with oxygen and hydroxyl groups on one lamellar face and silicon atoms coordinate tetrahedrically with oxygen atoms on the other lamellar face [14]. Adjacent layers are linked to one another by hydrogen bonds (Al–O–H···O–Si). These structural characteristics of kaolinite and its high surface area for adsorption of fluoride enable kaolinite to be an excellent carrier compared with the conventional SiO_2 filler used in composite resins. As NMF and DMSO are the most frequently used compounds for direct intercalation [14,22], we initially used these two solvents to expand the interlamellar structure of kaolinite. When the gallery space of kaolinite was intercalated by NMF or DMSO, the position of the characteristic peak of K-NMF or K-DMSO changed from $2\theta = 12.25°$ (Fig. 1a) to $2\theta = 8.1°$ (Fig. 1b) or $2\theta = 7.9°$ (Fig. 1c). The *d*-spacing (d_{001}) was also increased as shown in Table 1. It was noted that kaolinite had an inclined orientation in 001 reflections, and this behavior was related to the morphology of crystals that has been shown to grow in large and thin platelets [23]. Fig. 2a–f show the FTIR spectra of kaolinite, K-NMF, K-DMSO, K-diamine, K-acrylamide, and K-acetate, respectively. The bands at 3694, 3667, and 3650 cm^{-1} represent

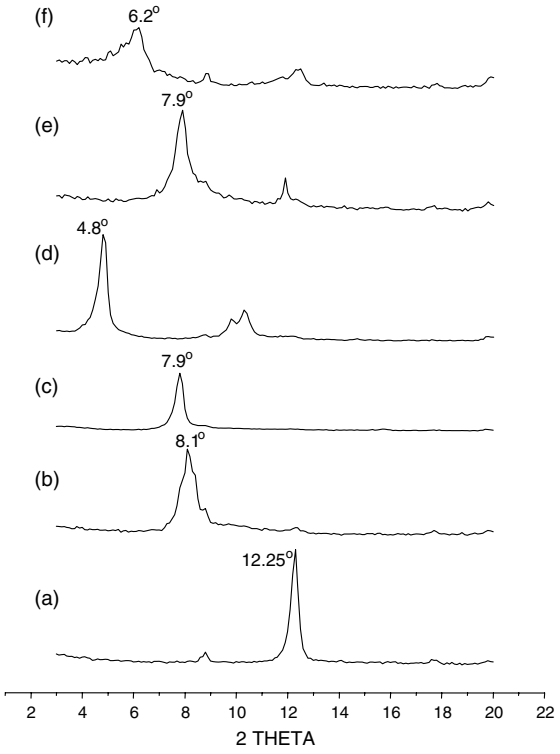

Fig. 1. X-ray diffraction pattern of: (a) kaolinite, (b) K-NMF, (c) K-DMSO, (d) K-diamine, (e) K-acrylamide, and (f) K-acetate.

Table 1
Determination of phases and *d*-spacing (d_{001}) (Å)

Phase	*d*-Spacings (Å)
Kaolinite	7.21
K-NMF	10.90
K-DMSO	11.18
K-Hexanediamine	18.39
K-acrylamide	11.19
K-ammonium acetate	14.21
C(K-hexanediamine)	18.39
C(K-acrylamide)	11.19
C(K-ammonium acetate)	14.21

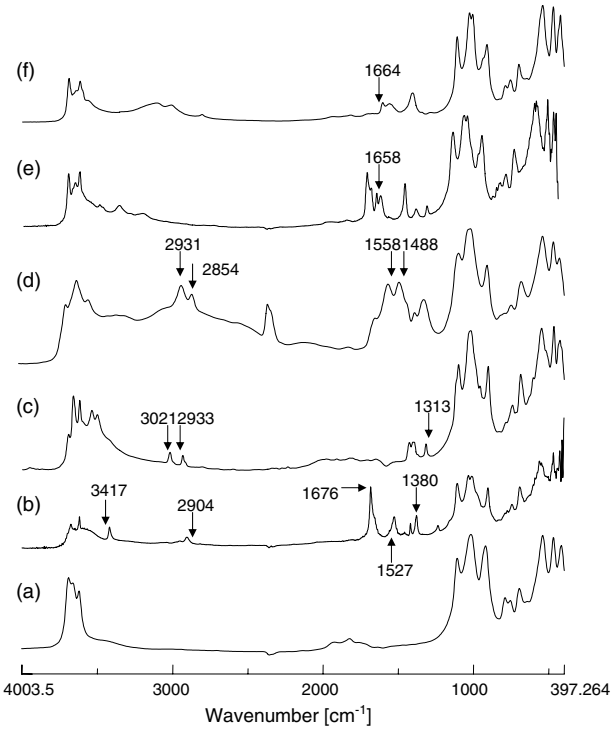

Fig. 2. X-ray diffraction pattern of: (a) C(K-diamine), (b) C(K-acrylamide), and (c) C(K-acetate).

the hydroxyl groups found in the surface of the kaolinite layered structure [24]. The band at 3622 cm^{-1} was attributed to hydroxyl groups that were embedded within the kaolinite matrix [25] (Fig. 2a). The FTIR spectra of K-NMF demonstrated many absorption bands at 1380 cm^{-1} (C═N), 1676 cm^{-1} (C═O), 1527 cm^{-1} (N–H), 2904 cm^{-1} (–CH_2–), and 3417 cm^{-1} (N–H) (Fig. 2b), which belong to the characteristic bands of NMF and were not observed in kaolinite. In addition, the bands representing the hydroxyl groups within the kaolinite matrix moved from 3622 to 3618 cm^{-1} and the hydroxyl groups in the surface of the kaolinite moved from 3694 to 3674 cm^{-1}, 3650 to 3647 cm^{-1}, and 917 to 912 cm^{-1} (Fig. 2b). Fig. 2c shows the FTIR spectrum of K-DMSO. The absorption bands at 3021 and 2933 cm^{-1} represent the vibration mode of –CH_3 while the band at 1313 cm^{-1} represent the vibration mode of >SO. No absorption bands belonging to the functional groups of DMSO were found in the FTIR spectrum of kaolinite (Fig. 2a). The localization of the intercalated molecules within the interlamellar structure of kaolinite is supported by the findings of XRD and FTIR analyses in this study. Our data suggest that NMF and DMSO were intercalated into the interlamellar space of kaolinite.

Because hexanediamine and ammonium acetate could enhance the adsorption of fluoride onto kaolinite [26] and the C═C double bond of acrylamide might interact with Bis-GMA, we selected hexanediamine and acrylamide to displace NMF and ammonium acetate to displace DMSO in this study. The hexanediamine-intercalated kaolinite (K-diamine) obtained from a gradual displacement of NMF exhibited a characteristic peak shift from $2\theta = 8.1°$ to $2\theta = 4.8°$ (Fig. 1d) as well as a lattice expansion from 10.90 to 18.39 Å (Table 1). After displacement of NMF by hexanediamine (Fig. 2d), the absorption bands of K-diamine displayed many characteristic peaks of hexanediamine such as 2931, 2854, 1488 (–CH_2–), and 1558 cm^{-1} (NH_2). No characteristic peaks of K-NMF were found in the FTIR spectrum of K-diamine. This confirmed the complete absence of any cointercalated NMF within the hexanediamine-intercalated kaolinite. In our preliminary study, hexanediamine could not be intercalated into a kaolinite host that kaolinite had not been preintercalated with NMF. Therefore, pretreatment with NMF was a requirement for the successful inclusion of hexanediamine. Similarly, K-acrylamide and K-acetate also demonstrated a shift of characteristic peaks, a lattice expansion in XRD analysis (Fig. 1e and f). When the NMF was displaced by acrylamide (Fig. 2e), a new band representing the absorption bands of C═C (1658 cm^{-1}) was found in the FTIR spectrum of K-acrylamide which was not found in that of K-NMF (Fig. 2b). In addition, the hydroxyl groups in the surface of the K-Acrylamide moved from 3674 to 3697 cm^{-1} and from 3647 to 3651 cm^{-1}. Finally, an absorption band belonging to R–COO^- (1664 cm^{-1}) was found in the FTIR spectrum of K-acetate (Fig. 2f) which could not be found in that of K-DMSO (Fig. 2c). Moreover, the characteristic absorption bands (3021, 2933, 1313 cm^{-1}) of K-DMSO were also not found in the FTIR spectrum of K-acetate, indicating DMSO was completely displaced by ammonium acetate.

Our TEM analysis indicated that the nano-particles including K-diamine, K-acrylamide, or K-acetate were polyhedral and 30–60 nm in size. When nanocomposite resins were prepared by mixing Bis-GMA, TEGDMA, DMPT, and camphorquinone with K-diamine, K-acrylam-

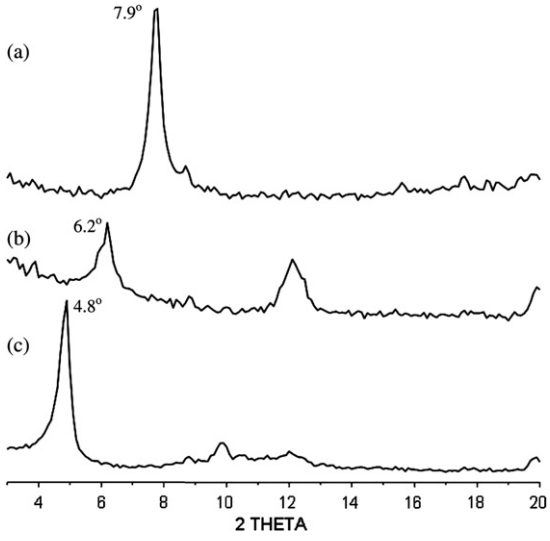

Fig. 3. FTIR spectra of: (a) kaolinite, (b) K-NMF, (c) K-DMSO, (d) K-diamine, (e) K-acrylamide, and (f) K-acetate.

ide, or K-acetate, the characteristic peaks did not change. This finding implied that these polymer additives formed composites with kaolinite and did not intercalate in the kaolinite (Fig. 3). The degree of polymerization of C(K-diamine), C(K-acrylamide), C(K-acetate), and Z-100 was 55%, 62%, 57%, and 64%, respectively. In addition, C(K-diamine), C(K-acrylamide), and C(K-acetate) appeared light yellow due to the inclusion of CQ before and after the 56-day release period.

3.2. Hardness, flexural strength, flexural modulus, fracture toughness, and diametral tensile strength measurements

The hardness, flexural strength, flexural modulus, fracture toughness, and diametral tensile strength of C(K-diamine), C(K-acrylamide), C(K-acetate), and Z-100 are listed in Table 2. Several commercial composite materials are included for comparison [27]. There was no significant difference in the values of these parameters between any two of the fabricated polymer–kaolinite nanocomposite resins. C(K-acrylamide) exhibited the greatest values while C(K-diamine) exhibited the lowest values. We hypothesized that the coupling between C=C double bond of acrylamide and Bis-GMA might facilitate stress transfer and reduce stress concentration along the interface of polymer–kaolinite, allowing for strength improvement [28]. Compared with the reported mechanical strengths of commercial product, the mechanical properties of C(K-acrylamide) were similar to those of Solitaire. The diametral tensile strengths of these polymer–kaolinite nanocomposite resins ranged from 31.7 to 35.3 MPa. As the American Dental Association has stipulated that tensile strengths of the composite resins for restorations must be greater than 34 MPa, only C(K-acrylamide) is suitable as a restorative material.

3.3. Fluoride release measurement

GICs can release the greatest amount of fluoride among currently available dental restorative materials. This is attributed to their acid–base reaction that can subsequently result in the leaching of fluoride [29]. However, GICs generally have low mechanical strengths, i.e. flexural strength: 41 MPa [30], and diametral tensile strength: 10.55 MPa [31]. In composites, the problem of limited fluoride release has yet to be overcome although the mechanical strength is sufficient for use in dentistry. In this study, Z-100, which includes no fluoride, was used as a negative control. There were significant differences between any two materials at all time points (Fig. 4). In addition, all of the fabricated polymer–kaolinite nanocomposite resins demonstrated a greater fluoride release than Fuji IX over a 56-day period (Fig. 4). This finding is attributable to the ability of many functional groups of kaolinite to adsorb fluoride. These groups include ·SiOH on the face of tetrahedral sheets, ·AlOH on the face of octahedral sheets, ·SiOH and ·AlOH at the edges of sheets, and Lewis acid sites along the edges of sheets [13]. Moreover, ·SiOH and ·AlOH located at the edges are the major sites for adsorption. The reaction mechanism was suggested as follows [13]:

$$> \mathrm{AlOH} + \mathrm{H^+} + \mathrm{F^-} \rightarrow > \mathrm{AlF} + \mathrm{H_2O}$$

$$> \mathrm{SiOH} + \mathrm{H^+} + \mathrm{F^-} \rightarrow > \mathrm{SiF} + \mathrm{H_2O}$$

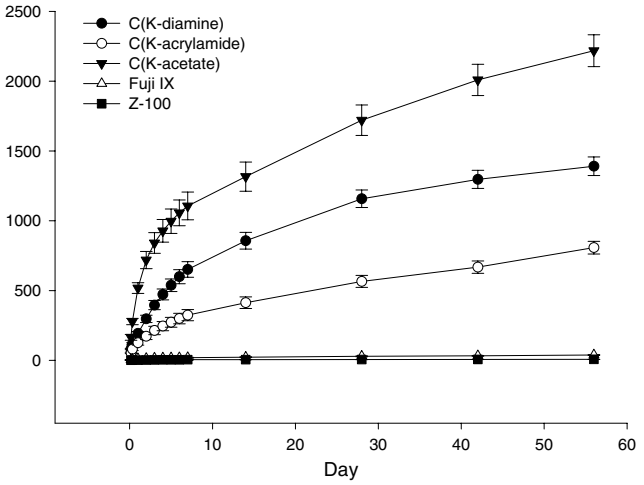

Fig. 4. Cumulative fluoride release of: C(K-diamine), C(K-acrylamide), C(K-acetate), GC Fuji IX, and Z-100 over a 56-day period ($n = 20$). There were significant differences between any two materials at all time points.

Table 2
The mechanical properties (mean ± standard deviation) of three polymer–kaolinite nanocomposite resins, Z-100, and commercial composite materials [27]

	Hardness	Flexural strength (MPa)	Flexural modulus (GPa)	Fracture toughness (MN $m^{-3/2}$)	Diametral tensile strength (MPa)
C(K-diamine)	42.2 (2.9)	74.2 (7.3)	4.0 (0.3)	1.1 (0.2)	31.7 (2.3)
C(K-acrylamide)	48.6 (2.2)	81.2 (9.4)	5.8 (0.4)	1.3 (0.2)	35.3 (1.9)
C(K-acetate)	44.3 (1.5)	77.2 (6.5)	4.3 (0.3)	1.2 (0.2)	32.5 (2.0)
Z-100	71.6 (3.2)	117.1 (10.2)	7.0 (0.7)	1.9 (0.2)	41.2 (2.2)
Alert	75.2 (10.9)	124.7 (22.1)	12.5 (2.1)	2.3 (0.2)	*
Surefil	70.4 (9.0)	132.0 (14.3)	9.3 (0.9)	2.0 (0.2)	*
Solitaire	41.7 (3.5)	81.6 (10.0)	4.4 (0.3)	1.4 (0.2)	*
Definite	65.8 (1.6)	103.0 (19.9)	6.3 (0.9)	1.6 (0.3)	*
Tetric Ceram	54.8 (1.1)	107.6 (11.4)	6.8 (0.5)	2.0 (0.1)	*
Ariston pHc	66.5 (2.6)	118.1 (10.5)	7.3 (0.8)	1.9 (0.2)	*

$n = 10$, *The value is not available in Ref. [27].

From the slope of Fig. 4, the greatest release of fluoride from polymer–kaolinite nanocomposite resins occurred during the first 7 days and then decreased with time. However, a stable release of fluoride was observed during the entire 56-day period. In contrast, Fuji IX had an initial high fluoride release for the first 3 days (i.e., the so-called "burst effect") which declined rapidly thereafter and then sustained at a lower level for the entire period. This phenomenon is similar to that of a previous study in which the release pattern was considered as probably owing to a hydrolysis process during the early period followed by a long-term diffusive process [4].

The rationale for fluoride exposure through restorative materials is its preventative value against caries. In this study, the cumulative fluoride release of the fabricated polymer–kaolinite nanocomposite resins after exposure to 0.2% NaF at pH 7 or pH 4 was still higher than that of Fuji IX and Z-100 (Figs. 5 and 6). C(K-acetate) had the greatest amount of fluoride release, however, C(K-acrylamide) had more cumulative fluoride release than C(K-diamine) after recharge. After exposure to 0.2% NaF solution at pH 7 for one minute, there were significant differences between any two materials at all time points except the two materials, C(K-diamine) and C(K-acrylamide), which exhibited no significant difference at all time points (Fig. 5). After exposure to 0.2% NaF solution at pH 4 for one minute, there were significant differences between any two materials at all time points except the two materials, C(K-diamine) and C(K-acrylamide), which exhibited no significant difference at 4, 8 h; 1, 2, 3, 4, 5, 6, 7, 14 days (Fig. 6). The results imply that the fluoride uptake capacity of these polymer–kaolinite nanocomposite resins was superior to that of Fuji IX and Z-100. The formation of fluoridated apatite is superior to CaF_2 in resisting caries progression,

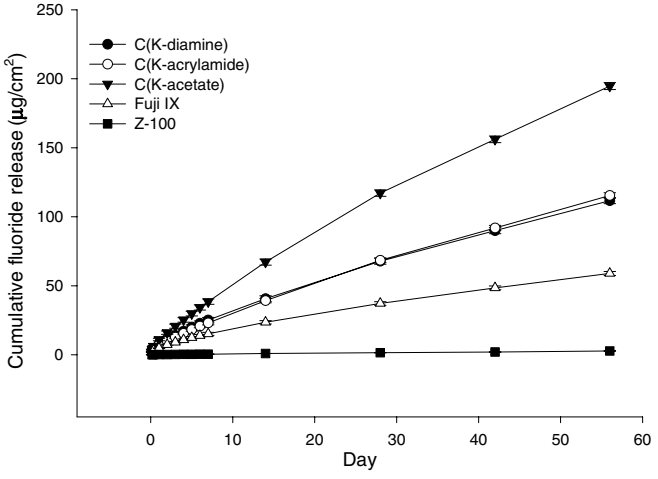

Fig. 5. Cumulative fluoride release of: C(K-diamine), C(K-acrylamide), C(K-acetate), GC Fuji IX, and Z-100 over a 56-day period after exposure to 0.2% NaF at pH 7 for 1 min ($n = 10$). There were significant differences between any two materials at all time points except the two materials, C(K-diamine) and C(K-acrylamide), which exhibited no significant difference at all time points.

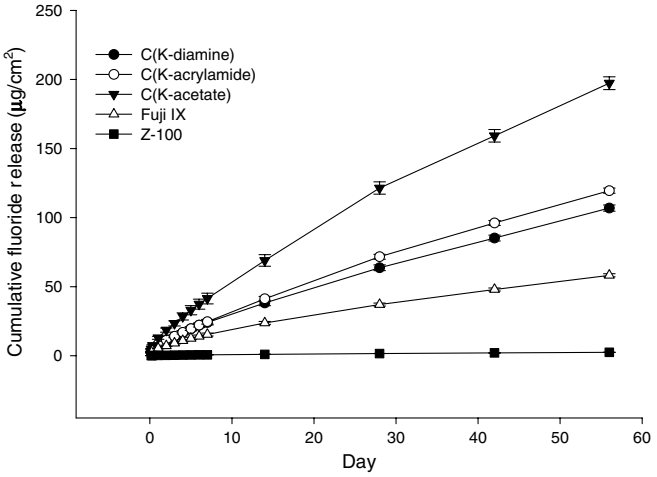

Fig. 6. Cumulative fluoride release of C(K-diamine), C(K-acrylamide), C(K-acetate), GC Fuji IX, and Z-100 over a 56-day period after exposure to 0.2% NaF at pH 4 for one minute ($n = 10$). There were significant differences between any two materials at all time points except the two materials, C(K-diamine) and C(K-acrylamide), which exhibited no significant difference at 4, 8 h; 1, 2, 3, 4, 5, 6, 7, 14 days.

and it can shift the condition of demineralization toward remineralization [32]. Whether the long-lasting fluoride release and recharge abilities of polymer–kaolinite nanocomposite resins can contribute to the formation of fluoridated apatite or CaF_2 on tooth surfaces requires further investigation.

4. Conclusion

This study demonstrated that hexanediamine-, acrylamide-, and ammonium acetate-intercalated kaolinite could be fabricated by the gradual displacement of NMF or DMSO. The fluoride release and recharge properties of C(K-acrylamide) were superior to those of Fuji IX and Z-100. These findings suggest that C(K-acrylamide) might be a useful dental restorative material with caries-preventive properties.

References

[1] Verbeeck RMH, De Moor RJG, Van Even DFJ, Martens LC. The short-term fluoride release of a hand-mixed vs. capsulated system of a restorative glass-ionomer cement. J Dent Res 1992;72:577–81.

[2] Itota T, Al-Naimi OT, Carrick TE, Yoshiyama M, McCabe JF. Fluoride release and neutralizing effect by resin-based materials. Oper Dent 2005;30:522–7.

[3] Okuyama K, Murata Y, Pereira PNR, Miguez PA, Komatsu H, Sano H. Fluoride release and uptake by various dental materials after fluoride application. Am J Dent 2006;19:123–7.

[4] Xu X, Burgess JO. Compressive strength, fluoride release and recharge of fluoride-releasing materials. Biomaterials 2003;24:2451–61.

[5] Savarino L, Breschi L, Tedaldi M, Ciapetti G, Tarabusi C, Greco M, et al. Ability of restorative and fluoride releasing materials to prevent marginal dentine demineralization. Biomaterials 2004;25:1011–7.

[6] Attar N, Onen A. Fluoride release and uptake characteristics of aesthetic restorative materials. J Oral Rehabil 2002;29:791–8.
[7] Eichmiller FC, Marjenhoff WA. Fluoride-releasing dental restorative materials. Oper Dent 1998;23:218–28.
[8] Burke FM, Ray NJ, McConnell RJ. Fluoride-containing restorative materials. Int Dent J 2006;56:33–43.
[9] Forsten L. Fluoride release and uptake by glass-ionomers and related materials and its clinical effect. Biomaterials 1998;19:503–8.
[10] Ten Cate JM, Featherston JDB. Physicochemical aspects of fluoride–enamel interactions. In: Fejerskov O, Ekstrand J, Burt BA, editors. Fluoride in dentistry. Copenhagen: Munksgaard; 1996. p. 252–72.
[11] Christoffersen J, Christoffersen MR, Arends J, Leonardsen ES. Formation of phosphate-containing calcium fluoride at the expense of enamel, hydroxyapatite and fluorapatite. Caries Res 1995;29: 223–30.
[12] Christoffersen J, Christoffersen MR, Kibalczyc W, Perdok WG. Kinetics of dissolution and growth of calcium fluoride and effects of phosphate. Acta Odontol Scand 1988;46:325–36.
[13] Weerasooriya R, Wickramarathne HUS, Dharmagunawardhane HA. Surface complexation modeling of fluoride adsorption onto kaolinite. Colloid Surface A 1998;144:267–73.
[14] Thompson JG, Cuff C. Crystal-structure of kaolinite–dimethylsulfoxide intercalate. Clays Clay Miner 1985;33:490–500.
[15] Ferracane JL, Greener EH. Fourier transform infrared analysis of degree of polymerization in unfilled resins – methods comparison. J Dent Res 1984;63:1093–5.
[16] International Standard Organization. ISO 4049-Dentistry: resin-based filling materials. Technical corrigendum, vol. 1. Switzerland: ISO; 1988.
[17] Srawley JE. Wide range stress intensity factor expressions for ASTM E-399 standard fracture toughness specimens. Int J Fracture 1976;12:475–6.
[18] Anderson TL. Fracture testing of nonmetals. In: Fracture mechanics. Fundamentals and applications. New York: Taylor & Francis; 2005. p. 353–84.
[19] Atai M, Nekoomanesh M, Hashemi SA, Amani S. Physical and mechanical properties of an experimental dental composite based on a new monomer. Dent Mater 2004;20:663–8.
[20] Hsu HM, Huang GF, Chang HH, Wang YL, Guo MK. A continuous flow system for assessing fluoride release/uptake of fluoride-containing restorative materials. Dent Mater 2004;20:740–9.
[21] Vogel GL, Chow LC, Brown WE. Microanalytical techniques with inverted solid state ion-selective electrodes. I. Nanoliter volumes. Analyt Chem 1980;52:375–7.
[22] Uwins PJR, Mackinnon IDR, Thompson JG, Yago AJE. Kaolinite–NMF intercalates. Clays Clay Miner 1993;41:707–17.
[23] Gardolinski JE, Carrera LCM, Cantao MP, Wypych F. Layered polymer–kaolinite nanocomposites. J Mater Sci 2000;35:3113–9.
[24] Olejnik S, Aylmore LAG, Posner AM, Quirk JP. Infrared spectra of kaolin mineral–dimethyl sulfoxide complexes. J Phys Chem 1968;72:241–8.
[25] Frost RL. Hydroxyl deformation in kaolins. Clays Clay Miner 1998;46:280–9.
[26] Crivello JV. Applications of photoinitiated cationic polymerization in coatings. J Coating Technol 1991;63:35–8.
[27] Manhart J, Kunzelmann K, Chen HY, Hickel R. Mechanical properties of new composite restorative materials. J Biomed Mater Res 2000;53:353–61.
[28] Lebaron PC, Wang Z, Pinnavaia TJ. Polymer-layered silicate nanocomposites: an overview. Appl Clay Sci 1999;15:11–29.
[29] Anusavice KJ. Phillips' Science of dental materials. Philadelphia: W.B. Saunders Company; 1996. pp. 273.
[30] Peez R, Frank S. The physical-mechanical performance of the new Ketac Molar Easymix compared to commercially available glass ionomer restoratives. J Dent 2006;34:582–7.
[31] Yap AU, Pek YS, Cheang P. Physico-mechanical properties of a fast-set highly viscous GIC restorative. J Oral Rehabil 2003;30:1–8.
[32] Featherstone JD, Glena R, Shariati M, Shields CP. Dependence of in vitro demineralization of apatite and remineralization of dental enamel on fluoride concentration. J Dent Res 1990;69:620–5.